Variable Connectivity Methods for the Atomistic Monte Carlo Simulation of Inhomogeneous and/or Anisotropic Polymer Systems of Precisely Defined Chain Length Distribution: Tuning the Spectrum of Chain Relative Chemical Potentials

Kostas Ch. Daoulas,[†] Andreas F. Terzis,[‡] and Vlasis G. Mavrantzas*[,†]

Institute of Chemical Engineering and High-Temperature Chemical Processes, ICE/HT-FORTH, GR 26500, Patras, Greece, and Department of Physics, University of Patras, GR 26500, Patras, Greece

Received October 9, 2002; Revised Manuscript Received May 27, 2003

ABSTRACT: Application of variable connectivity Monte Carlo (MC) methods to the simulation of atomistically detailed polymer melts leads to deviations from monodispersity. To control the chain length distribution, a spectrum $\boldsymbol{\mu}^*$ of chain relative chemical potentials needs to be applied. The spectrum $\boldsymbol{\mu}^*$ that produces the most common limiting molecular weight (MW) distributions has been obtained in the past only for polymers in the bulk, for which $\boldsymbol{\mu}^*$ is solely determined by combinatorial considerations. In this work, the methodology is extended to more complex systems, such as inhomogeneous and/or anisotropic polymer melts, by presenting a novel numerical scheme for deriving the relationship between $\boldsymbol{\mu}^*$ and desired chain length distribution, where the energetics of the system is also taken into account. We illustrate the new approach in the case of polymer melts grafted on a solid substrate (both for single and bulk chains), for which the relationship between $\boldsymbol{\mu}^*$ and actual chain length distribution proposed so far in the literature for free melts breaks down. In contrast, the new method correctly accounts for the effect of grafting on system polydispersity. This is verified in end-bridging Monte Carlo (EBMC) simulations of two polydisperse polyethylene (PE) melt systems, C_{78} and C_{156}, grafted on a noninteracting, hard surface at various grafting densities σ, for the case where the chain length distribution is constrained to be uniform or for the case where $\boldsymbol{\mu}^* = 0$. The new method allows extending and consistently applying newly developed chain connectivity-altering MC algorithms to the atomistic simulation of a variety of polymer melts where polydispersity should be precisely known.

1. Introduction and Motivation

Chain-connectivity altering methods such as end-bridging,[1,2] double bridging,[3] and intramolecular double rebridging[3] constitute the most powerful MC algorithms nowadays for the fast and efficient simulation of atomistically detailed polymer melts. All these moves tunnel through energetic barriers in the configurational space of the polymer, and allow for drastic structural rearrangements at the level of the chain end-to-end vector. Consequently, they lead to fast equilibration of the simulated system, which cannot thermally equilibrate by other means, thus circumventing the limitations imposed by the problem of long relaxation times in dynamic algorithms.[4,5] Thanks to these moves, long-chain polymer melts, such as polyethylene, polypropylene, and *cis*-1,4 polyisoprene, have been simulated today in full atomistic detail enabling the study of their structural, thermodynamic, and viscoelastic properties from first principles. More recently, the new moves have successfully been applied to the simulation of the interfacial properties of end-grafted polymer melts on a solid substrate, such as graphite.[6]

In their majority, chain connectivity-altering MC moves induce fluctuations in the chain length distribution and lead to deviations from monodispersity. A multicomponent (polydisperse) system is thereby obtained whose components differ from each other in degree of polymerization. During the simulation, the MW distribution can change from realization to realization; however, the average distribution can be controlled by specifying its conjugate variable, i.e., the spectrum $\boldsymbol{\mu}^*$ of chemical potentials of all chain lengths present except two that are considered to be reference species. The original formulation of variable connectivity methods for atomistically detailed polymer models was presented by Pant and Theodorou[1] in a *semigrand* statistical ensemble in which the parameters specified are: the total number of monomers or united atoms n, the total number of chains N_{ch}, the system temperature T and pressure P, and the spectrum $\boldsymbol{\mu}^*$ of reduced chemical potentials specifying the molecular length distribution. The spectrum $\boldsymbol{\mu}^*$ was defined according to

$$N_k = cy^{M_k} \exp(\beta\mu^*_k),\ (k = 1, \ldots, m,\ k \neq i, j)$$
$$N_i = cy^{M_i}, \quad N_j = cy^{M_j} \tag{1}$$

where N_k denotes the number of chains of species k, M_k is their molecular length, (i,j) is an arbitrary pair of chain lengths chosen as reference species, $\beta = 1/k_B T$, where k_B is Boltzmann's constant, and μ^*_k denotes the relative chemical potential of a chain of length M_k. Parameters c and y are Lagrange multipliers defined from the requirements of total chain and total monomer numbers constancy.

Pant and Theodorou[1] derived and tested expressions for the spectrum $\boldsymbol{\mu}^*$ that for a *bulk melt* (i.e., away from solid boundaries) at equilibrium reproduces all popular limiting chain length distributions; examples include the most probable, the uniform and the Gaussian

* To whom correspondence should be addressed at ICE/HT-FORTH. E-mail: vlasis@iceht.forth.gr. Telephone: (+30) 2610-965 214. Fax: (+30) 2610-965 223.
[†] ICE/HT-FORTH.
[‡] University of Patras.

10.1021/ma021570h CCC: $25.00
Published on Web 07/24/2003

distributions.[1] In all cases, however, the derivation was restricted to systems for which the system configurational integral in the canonical partition function exhibits a dependence only on monomer density and number-averaged MW, and not on the details of the distribution. As noted by Pant and Theodorou, when this condition is satisfied, the MW distribution is related to the spectrum $\boldsymbol{\mu}^*$ of chemical potentials solely by combinatorial considerations such that the energetics of the system can be neglected. For bulk systems away from any boundaries and in the absence of an externally imposed field, this is a true assumption provided short-chain species are absent. Consequently, all subsequent atomistic MC simulations with chain connectivity-altering moves, such as the end-bridging (EB) and the more advanced double-bridging (DB) and intramolecular double rebridging (IDR) moves,[3] have so far been executed with the spectrum $\boldsymbol{\mu}^*$ derived by Pant and Theodorou for a system of noninteracting unperturbed chains under the assumptions stated above. More specifically, the spectrum $\boldsymbol{\mu}^*$ that reproduces a uniform chain length distribution of width $2\psi\tilde{N}+1$ centered at the number-averaged degree of polymerization $\tilde{N}$ between a lower and a higher chain length has always been employed in the simulations:

$$\mu_k^* = \begin{cases} 0 & \text{for } M_{\text{low}} \le M_k \le M_{\text{high}},\ M_k \neq M_i,\ \ M_k \neq M_j \\ -\infty & \text{otherwise} \end{cases} \tag{2}$$

where $M_{\text{low}} = (1-\psi)\tilde{N}$ and $M_{\text{high}} = (1+\psi)\tilde{N}$ are the shortest and longest chain lengths allowed in the system with M_i, M_j ($M_{\text{low}} \le M_i < M_j \le M_{\text{high}}$) denoting the reference species lengths. The resulting distribution of chain lengths in this case is

$$\frac{N_k}{N_{\text{ch}}} = \begin{cases} \dfrac{1}{2\psi\,\tilde{N}+1}, & \text{for } M_{\text{low}} \le M_k \le M_{\text{high}} \\ 0, & \text{otherwise} \end{cases} \tag{3}$$

It is with the spectrum $\boldsymbol{\mu}^*$ of eq 2 that the recent atomistic EBMC simulations of structural and viscoelastic properties of a number of linear polymer melts (e.g., PE, PP, and *cis*-1,4 PI) have been carried out.

Equation 2 was in fact proven to keep the MW distribution uniform not only in simulations with equilibrium systems but also in simulations with systems beyond equilibrium such as in the case of a polymer melt subjected to a tensorial orienting field. For example, in the field-on (elasticity) EBMC simulations carried out by Mavrantzas and Theodorou[7] and Mavrantzas and Öttinger,[8] it was observed that a uniaxial elongational field $\boldsymbol{\alpha}$ that couples with the chain end-to-end vector conformation tensor $\mathbf{C}$ has no effect on the chain length distribution: for all fields $\boldsymbol{\alpha}$ investigated, the distribution remained uniform, exactly as in the corresponding equilibrium melts. This result should be considered as rather fortuitous, since in the original formulation of the $\boldsymbol{\mu}^*$ profile of eq 2 no field energy had been included in the configurational integral. Although this suggests that the assumption of a uniform distribution of chain lengths is consistent with the state of minimum free energy for the homogeneously deformed polymer melt under the applied tensorial field $\boldsymbol{\alpha}$, such a conclusion should not be taken as general. From the point of view of statistical mechanics, for a given set $\boldsymbol{\mu}^*$ of chain relative chemical potentials, there must exist a preferred MW distribution subject to the macroscopic restrictions realized in the semigrand ensemble.

A case where the strong interplay between macroscopic restrictions and resulting MW distribution immediately manifests itself is in model systems of terminally anchored polymer melts. As will be shown in detail in this paper, by naive employment in simulations with *end-grafted melts* the spectrum $\boldsymbol{\mu}^*$ of eq 2, the resulting chain length distribution is definitely nonuniform. Further, it strongly depends on the value of grafting density σ assumed in the simulation: it favors the smaller and longer chain lengths allowed, particularly at the highest grafting densities where the brush becomes essentially bimodal. In practice, polydispersity in MW of commercial-grade polymers is ubiquitous and is often used to tailor brush properties. An understanding of the factors and mechanisms governing MW distribution and their effect on the equilibrium statistics of a grafted polymer melt is therefore highly desirable, since it can facilitate the rational design of materials with optimal properties.

It is the purpose of this paper to develop an efficient methodology for defining the spectrum $\boldsymbol{\mu}^*$ of chain relative chemical potentials that should be specified in atomistic simulations of multicomponent systems where both entropic and enthalpic factors influence their properties such that the resulting MW is precisely controlled. The methodology is general enough and can be applied to any model polymer system, where polydispersity should be strictly preserved. The paper is organized as follows: section 2 focuses on the resulting MW distribution in a grafted polymer melt for the spectrum of reduced chemical potentials specified by eq 2. Section 3 presents the methodology for deriving the relationship between spectrum $\boldsymbol{\mu}^*$ and chain length distribution for any inhomogeneous and/or anisotropic polymer melt and its implementation in atomistic simulations through an efficient iterative numerical scheme. Illustrations of the new modeling scheme are given in section 4, which presents results from EBMC simulations with multicomponent grafted polymer melts of (a) noninteracting molecules modeled as freely jointed chains and (b) bulk chains that validate the new method. Conclusions and plans for future work are discussed in section 5.

2. A Recent Atomistic EBMC Simulation and the Resulting MW Distribution

In a recent study,[6] a computer simulation technique was developed that is capable of probing the structure of the interface between a solid substrate and a long polymer melt consisting of grafted chains, or a mixture of free and grafted chains, at a prescribed grafting density σ. The interface between bulk PE melt and a graphite basal plane or a noninteracting hard surface (i.e., a wall) was considered. Two PE systems, a C_{78} and a C_{156} melt, were simulated, at grafting densities σ ranging from 1.31 to 2.62 nm^{-2} and values of the polydispersity parameter ψ between 0.8 and 0.9 (corresponding to polydispersity indices $I = 1.21$ to 1.26, respectively). The simulations were executed with the united-atom model of ref 2 by using the profile of chemical potentials $\boldsymbol{\mu}^*$ described by eq 2. [As noted above, for a melt of nongrafted chains (free melt), such a spectrum reproduces a uniform distribution of chain lengths.] Atomistic-level information concerning the

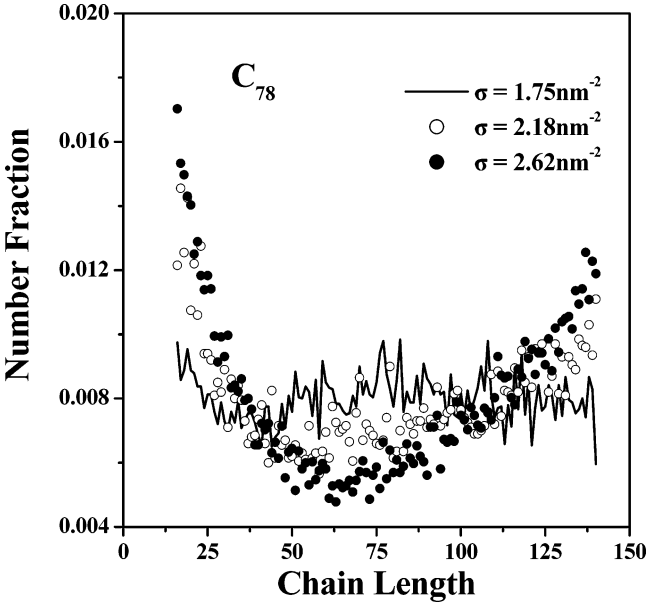

Figure 1. Molecular length distribution in the polydisperse C_{78} polymer melt ($T = 450$ K, $P = 0$ atm, $\psi = 0.8$) for $\mu^* = 0$, as a function of grafting density σ.

conformational (chain orientation and packing), thermodynamic (local density, segment profiles belonging to free and adsorbed chains, distributions of chain ends), and structural (bond ordering, ^{2}H NMR spectrum) properties of the two melts near the solid substrate have been published in two recent papers.[6,9] In the next paragraphs of this section, additional results are presented concerning the resulting MW distribution in the two melts.

For the grafted C_{78} PE melt (characterized by $\psi = 0.8$), the resulting MW distribution is presented in Figure 1, as a function of grafting density σ. It is observed that, with increasing grafting density, the distribution presents systematic deviations from the uniform profile exhibiting maxima at the lower and higher molecular lengths allowed in the simulation and minima at the intermediate ones. The degree of nonuniformity appears to be higher for the larger σ value studied ($\sigma = 2.62$ nm^{-2}); for this grafting density, the fraction of shortest and longest chains almost doubles relative to the uniform polydispersity case, with the melt becoming essentially a bimodal polymer mixture. This is schematically shown in Figure 2 presenting an atomistic snapshot of the melt at the end of the EBMC simulation, when thermodynamic equilibrium is achieved. Chains with molecular lengths higher than 60 are shaded in dark green whereas chains with molecular lengths lower than 60 are shaded in red. The bimodal-like configuration of the melt due to stratification of the locations of the free ends above the grafting surface shows up quite evidently.

Similar plots are obtained for the grafted C_{156} PE melt shown in Figure 3. Again, for a similar value of the polydispersity parameter ψ (=0.9), the degree to which the molecular length distribution deviates from the uniform profile increases with increasing σ. This behavior was seen to persist irrespective of the width of the distribution function.

To analyze the origin of the tendency of the grafted melt to separate and take the form of a bimodal-like brush, we carried out additional MC simulations of the C_{78} and C_{156} systems modeled as freely jointed and/or

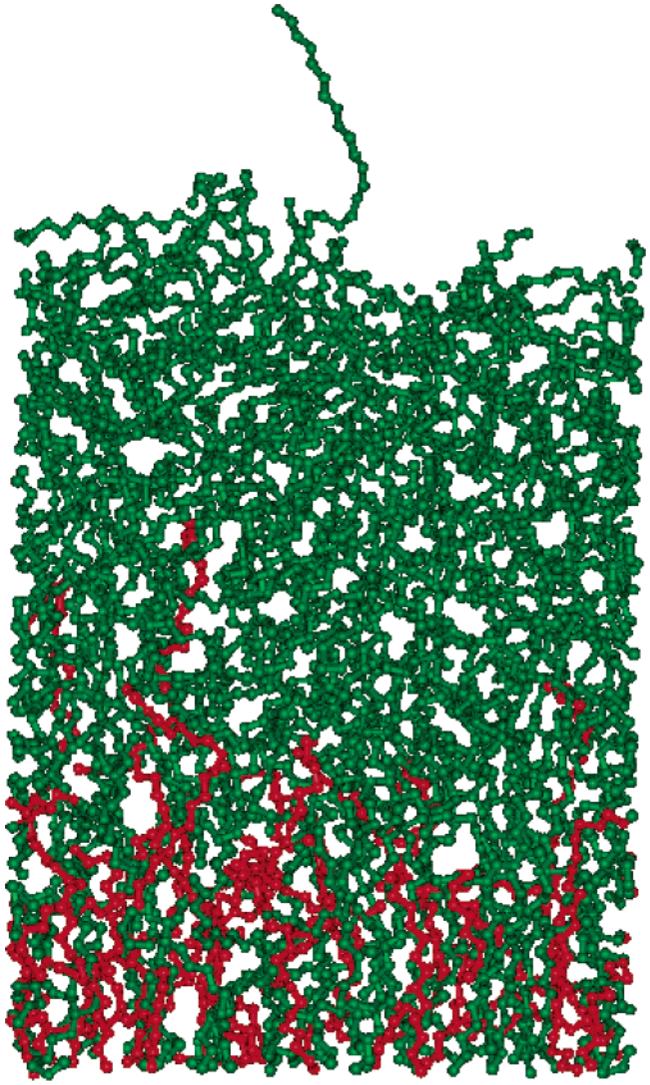

Figure 2. Atomistic snapshot of the polydisperse C_{78} polymer melt grafted at $\sigma = 2.62$ nm^{-2}, at a state of thermodynamic equilibrium ($T = 450$ K, $P = 0$ atm, $\psi = 0.8$, $\mu^* = 0$). Chains with molecular length higher than 60 are shaded in dark green whereas those with molecular length lower than 60 are shaded in red.

phantom chains. Phantom chains are defined as isolated chains governed only by the bending potential of the corresponding bulk chains. MC simulations of freely jointed and phantom chains are much less demanding computationally than those of melt systems; therefore, they permit a more accurate prediction of the resulting MW distribution. For the C_{78} melt (polydispersity parameter $\psi = 0.8$), the MW distributions obtained from the simulations with these two models are shown in Figure 4a, and, interestingly enough, they are also seen to be nonuniform; they are further seen to coincide. Since no *mer−mer intermolecular interactions* are considered in the MC simulations with these two models, it is immediately recognized that the origin of the MW nonuniformity for single chains is entropic: it is related to the lower entropy loss experienced by the shorter chains confined above the grafting plane relative to longer ones. For grafted melts in the bulk where mer−mer intermolecular interactions are present, enthalpic contributions leading to chain stretching are added to the entropic contribution, thus enhancing the extent of nonuniformity. Also shown in Figure 4a is the corresponding MW distribution (for $\mu^* = 0$) for single grafted

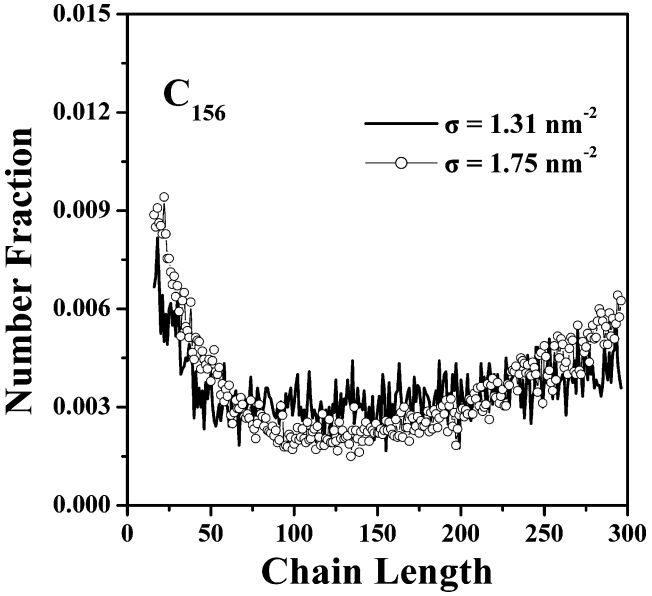

Figure 3. Same as in Figure 1 but for the polydisperse (ψ = 0.9) C_{156} grafted polymer melt.

chains derived analytically through a theory which will be described in detail in section 4.1.

The above examples demonstrate that the expressions proposed by Pant and Theodorou[1] for the relationship between chemical potential spectrum $\boldsymbol{\mu}^*$ and generated chain length distribution are strictly valid only in systems of noninteracting (i.e., unperturbed) *free* chains, due to consideration of merely combinatorial effects. In anisotropic or inhomogeneous polymer systems, however, the relative effect of energetics should also be addressed; otherwise the prescribed recipes for $\boldsymbol{\mu}^*$ may be faulty. Section 3 below proposes a new methodology for deriving the correct relationship between system polydispersity and chemical potential spectrum $\boldsymbol{\mu}^*$ for any polymer system, and section 4 validates it in simulation studies of multicomponent grafted systems with both single-unperturbed and bulk chains.

3. A Generalized Relationship between Chain Length Distribution and Spectrum $\boldsymbol{\mu}^*$

Following the methodology introduced by Pant and Theodorou,[1] the natural thermodynamic potential to consider for the variables of interest [$N_{ch}nVT\boldsymbol{\mu}^*$] is

$$Y = F - \sum_{\substack{k=1 \\ k\neq i,j}}^{m} \mu^*_k N_k \tag{4}$$

where F is the Helmholtz energy of the m-component mixture (k = 1, 2, .., m), N_k stands for the number of chains of species k (characterized by length M_k), (i,j) is the selected arbitrary pair of reference species (of lengths M_i and M_j, respectively) for which $\mu^*_i = \mu^*_j = 0$, n the total number of atoms and N_{ch} the total number of chains in the system [for consistency, the notation introduced by Pant and Theodorou is also kept here]. Y is related to a partition function $\tilde{Y}$ through

$$Y = -k_B T \ln \tilde{Y} \tag{5}$$

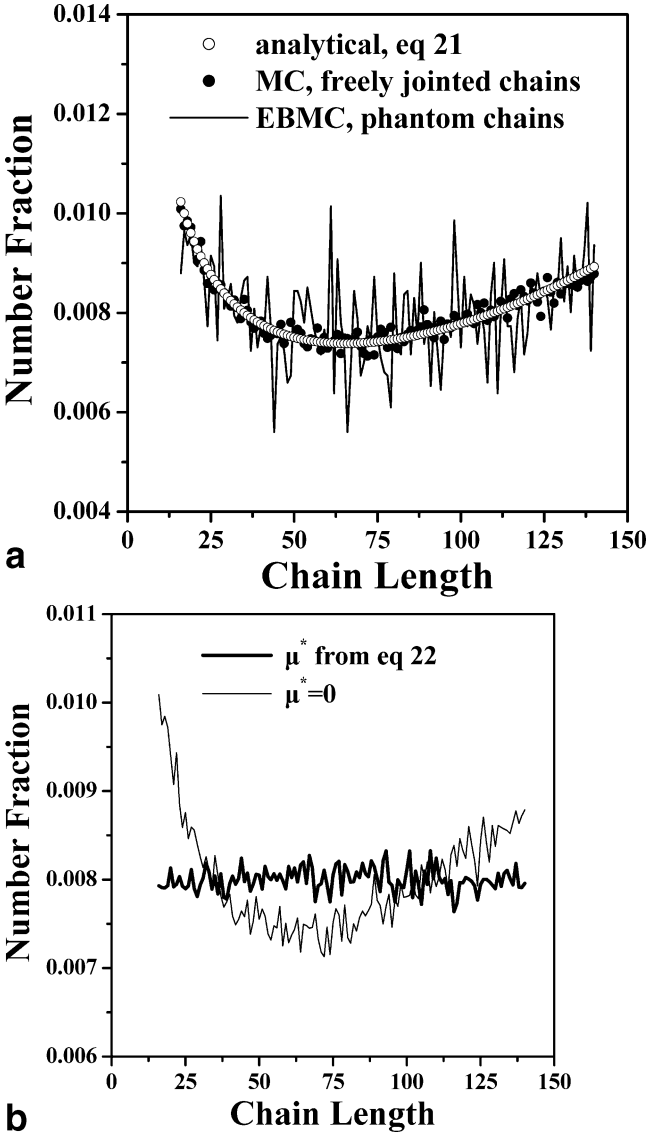

Figure 4. (a) Chain length distribution in a polydisperse system of single noninteracting C_{78} chains (T = 450 K, ψ = 0.8, $\boldsymbol{\mu}^* = 0$) grafted on a hard surface as obtained from EBMC simulations with phantom chains (continuous line) and MC simulations with freely jointed chains (filled circles) and as calculated analytically with eq 21 (open circles). (b) Comparison of the chain length distributions obtained from MC simulations with freely jointed chains using the spectrum $\boldsymbol{\mu}^*$ of eq 22 (thick line) and the spectrum $\boldsymbol{\mu}^* = \mathbf{0}$ (thin line) [C_{78} chains, ψ = 0.8]. It is seen that eq 22 indeed generates a uniform distribution of chain lengths.

where

$$\tilde{Y}[N_{ch},n,V,T,\mu^*] = \sum_{\{N_1,\ldots,N_m\}} \exp[\beta \sum_{\substack{k=1 \\ k\neq i,j}}^{m} \mu^*_k N_k] Q(V,T,N_1,\ldots,N_m) \tag{6}$$

and the summation is restricted over those chain length distributions for which

$$\sum_{k=1}^{m} M_k N_k = n, \quad \sum_{k=1}^{m} N_k = N_{ch} \tag{7}$$

In the above equations, $Q(V,T,N_1,N_2,\ldots,N_m)$ is the canonical partition function for the m-component system

given by

$$Q(V,T,N_1,...,N_m) = \frac{N_{ch}!}{N_1!N_2!...N_m!}\frac{1}{\Lambda^{3n}}Z(V,T,N_1,...,N_m) \quad (8)$$

where $Z(V,T,N_1,...,N_m)$ denotes the classical configurational integral and Λ the mer wavelength. Q is linked to the Helmholtz energy of the system through

$$F = -k_B T \ln(Q) \quad (9)$$

Equation 6, combined with the constraints of eq 7, is the starting point for deriving the relationship between spectrum $\boldsymbol{\mu}^*$ and chain length distribution for any model polymer system. A significant role in this derivation is played by the configurational integral $Z(V,T,N_1,...,N_m)$ defined through

$$Z(V,T,N_1,...,N_m) = \int d^{3n}r \exp[-\beta V(\mathbf{r}_1,...,\mathbf{r}_n)] \quad (10)$$

with the potential energy function $V(\mathbf{r}_1, \mathbf{r}_2, ..., \mathbf{r}_n)$ incorporating all system energetics due to bonded and nonbonded interactions. For noninteracting systems, Pant and Theodorou assumed that the configurational integral depends only on the total number of chains N_{ch} and monomers n and *not* on the exact form of the chain length distribution, i.e.: $Z(V,T,N_1,...,N_m) = Z(V,T,n,N_{ch})$. Simulation results justified the validity of such an assumption also for free polymer melts in the bulk, but the results of section 2 of this paper demonstrated its invalidity for systems of terminally anchored polymer melts. How to relax the assumption by quantifying the strong dependence of Z on the details of the MW distribution is the subject of the remaining of this section.

The starting point is the expression for the Helmholtz free energy F of the system

$$F = F_0 + (F - F_0) = F_0 + \Delta F \quad (11)$$

where F_0 denotes the free energy of the reference homogeneous or isotropic melt characterized by the same number of chains N_{ch}, the same total number of mers n and the same molecular length distribution N_1, N_2, ..., N_m as the inhomogeneous melt. For example, for a grafted melt, F_0 is the free energy of the corresponding free melt. F_0 is defined as

$$\beta F_0 = -\ln\left(\frac{N_{ch}!}{N_1!...N_m!}\right) - \ln\left(\int d^{3n}r \exp[-\beta V(\mathbf{r}_1, ..., \mathbf{r}_n)]\right) \quad (12)$$

Furthermore, following the arguments of Pant and Theodorou,[1] for a free melt, the second term on the right-hand-side of the equation does not depend on the details of the MW distribution, and can be considered as a constant. To within this constant and having introduced the quantity $\Delta F = F - F_0$, the partition function $\tilde{Y}$ of the melt is then written as

$$\tilde{Y} = \sum_{\{N_1,N_2,...,N_m\}} \frac{N_{ch}!}{N_1!...N_m!} \exp(\beta \sum_{j=1}^{m} \mu_j^* N_j - \beta \Delta F) \quad (13)$$

Substituting eq 13 into eq 5 for the thermodynamic potential Y (the analogue of Gibbs energy in the semi-grand ensemble of Pant and Theodorou[1]), invoking a maximum term approximation on $\ln(\tilde{Y})$, subject to the two constraints of eq 7, and using Stirling's approximation for the logarithms of factorial terms, we found the relation between specified chain chemical potential and chain length distribution by minimizing the functional

$$\tilde{G} = \sum_{j=1}^{m} N_j - \sum_{j=1}^{m} N_j \ln(N_j) + \lambda\left(\sum_{i=1}^{m}\frac{N_i M_i}{N_{ch}} - \tilde{N}\right) + \eta\left(\sum_{i=1}^{m}\frac{N_i}{N_{ch}} - 1\right) + \beta\left(\sum_{i=1}^{m}\mu_i^* N_i - \Delta F\right) \quad (14)$$

where λ and η are the Lagrange multipliers associated with the constraints of eq 7. The minimization leads to the following set of algebraic equations:

$$\sum_{k=1}^{m} M_k N_k = n$$

$$\sum_{k=1}^{m} N_k = N_{ch} \quad (15)$$

$$\ln(N_k) + \beta\frac{\partial \Delta F}{\partial N_k} - \lambda\left(\frac{M_k}{N_{ch}}\right) - \eta\left(\frac{1}{N_{ch}}\right) - \beta\mu^*{}_k = 0, \quad k = 1, ..., m$$

This is the main result of the present work: For given values of the spectrum $\boldsymbol{\mu}^*$, eq 15 can be solved to yield the resulting distribution of chain lengths and vice versa, if the partial derivatives $\partial\Delta F/\partial N_k$ were known.

Unfortunately, ΔF is usually a complicated function of the chain length distribution whose estimation, even for simple systems, could be a formidable task. Even if analytical expressions are available, the approximations made during their derivation could result in inaccurate $\boldsymbol{\mu}^*$-MW relationships.

It turns out, however, that the partial derivatives $\partial\Delta F/\partial N_k$ entering eq 15 can be accurately calculated through a stochastic (e.g., MC) simulation by analyzing the MW chain length distribution at prescribed $\boldsymbol{\mu}^*$ values according to the following combined stochastic-numerical iterative scheme.

Step 1: Use the spectrum $\boldsymbol{\mu}^*$ proposed by Pant and Theodorou as an initial guess to start the simulations. From the *resulting* chain length distribution (which may not be the desired one), calculate the values of the partial derivatives $\partial\Delta F/\partial N_k$ using eq 15 and the initial $\boldsymbol{\mu}^*$ spectrum.

Step 2: Insert the values of $\partial\Delta F/\partial N_k$ obtained at the end of the first step and the *prescribed* chain length distribution into eq 15 and solve it to get an improved spectrum $\boldsymbol{\mu}^*$.

Step 3: Use the improved $\boldsymbol{\mu}^*$ profile in the MC algorithm and repeat the simulation to get a better approximation for the chain length distribution. If this matches the prescribed one, the procedure is finished. If not, the iterations are repeated until convergence is achieved, i.e., until a spectrum $\boldsymbol{\mu}^*$ is specified such that the chain length distribution that results from the MC simulation and the prescribed one match each other.

As stated, although the proposed scheme applies to any polymer system, there are cases where the function ΔF can be analytically calculated by thermodynamic arguments. A typical example is a system of single unperturbed molecules grafted at a distance z_0 above a

hard substrate, modeled as freely jointed chains. In this case, inserting the analytically calculated function ΔF into eq 15 leads directly to the spectrum $\boldsymbol{\mu}^*$, which should be specified in the simulation in order to fix the chain length distribution. On the other hand, there exist approximate expressions for the function ΔF, obtained, for example, through self-consistent mean-field (SCF) theories at a mesoscopic level. A typical example is the brush theories of Milner et al.[10] and Birshtein et al.,[11] which derive an analytical expression for the free energy of a polydisperse grafted melt relative to the free system as a function of grafting density, mean chain length, and molecular length distribution. In this case, the above modeling scheme can be used to test the accuracy of the analytical theory. Both of these cases are elaborated in the Examples section discussed below.

4. Examples

4.1. Noninteracting Grafted Chains. Noninteracting grafted chains are modeled here as freely jointed chains, since the corresponding model can be solved analytically. Following the diffusion equation approach[12,13] for the propagator $G(\mathbf{R},M_i)$ (the un-normalized probability density function that the end-to-end vector of an M_i segment long chain is $\mathbf{R}$ within d$\mathbf{R}$), the partition function $\tilde{Z}$ of a chain of length M_i grafted at position z_0 above the grafting plane, satisfying the *adsorbing boundary condition*,[12,13] is given by

$$\tilde{Z}(M_i) = \mathrm{erf}\left(\frac{\sqrt{3}z_o}{\sqrt{2M_i a^2}}\right) \tag{16}$$

which suggests that

$$\tilde{Z}(M_i) \underset{z_o \to 0}{\approx} \sqrt{\frac{6}{\pi a^2}}\frac{z_o}{\sqrt{M_i}} = C\frac{z_o}{\sqrt{M_i}} \tag{17}$$

where C is a numerical constant. Clearly, $\tilde{Z}$ depends on chain length M_i. Equations 16 and 17 give the partition function of a single end-grafted chain. For a polydisperse system of N_{ch} grafted chains where the allowed molecular lengths vary between M_{low} and M_{high} (so that the mean chain length is fixed, equal to $\tilde{N}$), the system partition function Z is given by the product of $\tilde{Z}$'s of individual molecular lengths:

$$Z(N_1,N_2,...,N_m) = C^{N_{ch}}\prod_{i=1}^{m}\left(\frac{z_o}{\sqrt{M_i}}\right)^{N_i} \tag{18}$$

where $M_1 = M_{low}$, $M_2 = M_{low} + 1$, ..., $M_m = M_{high}$, or, equivalently,

$$\Delta F = -k_B T\sum_{i=1}^{m} N_i \ln(\tilde{Z}(M_i)) \tag{19}$$

Substituting eq 19 into eq 15, the following equation is derived for the relationship between chain length distribution and spectrum $\boldsymbol{\mu}^*$:

$$\ln(N_k) + \frac{1}{2}\ln(M_k) + \lambda M_k + \eta - \beta\mu^*_k = 0 \tag{20}$$

Since the allowed molecular lengths vary between M_{low} and M_{high} (i.e., $M_1 = M_{low}$, ..., $M_m = M_{high}$) the number of possible different chain lengths is equal to ($M_{high} - M_{low} + 1$), while the index k varies in the interval [1, m] where $m = M_{high} - M_{low} + 1$. The two additional unknown parameters λ and η in eq 20 are the Lagrange multipliers associated with the constraints of eq 7.

Equation 20 is the desired relationship between chain length distribution and spectrum $\boldsymbol{\mu}^*$, and can be viewed in two ways: First, for a specified $\boldsymbol{\mu}^*$ profile, it determines the chain length distribution that should be expected at the end of the simulation. For example, the simulation data presented in section 2 for the freely jointed chain model were obtained by employing eq 2 for $\boldsymbol{\mu}^*$ in the MC simulation. Substituting eq 2 into eq 20, we see that the resulting MW distribution should be

$$N_m = \frac{C_1 \exp(C_2 M_m)}{\sqrt{M_m}} \tag{21}$$

with $M_1 = M_{low}$, $M_2 = M_{low} + 1$, ..., $M_m = M_{high}$; the two constants C_1 and C_2 should be fixed through eq 7. For $\tilde{N} = 78$ and $\psi = 0.8$ (i.e., $M_{low} = 16$ and $M_{high} = 140$), the chain length distribution obtained by eq 21 is plotted in Figure 4a by the open circles. Also shown in the same figure are the molecular length distributions discussed in section 2 (directly obtained from the MC simulations with the freely jointed and the phantom chain models). Expected and calculated chain length distributions clearly coincide, which proves the validity of our analysis.

Second, it allows one to analytically map several limiting chain length distributions onto spectra of chain relative chemical potentials. To generate, for example, a uniform distribution of chain lengths in the interval of width $2\psi\tilde{N} + 1$ centered at the number-averaged degree of polymerization $\tilde{N}$ (see eq 3), the chemical potential specification should be

$$\beta\mu^*_k = \begin{cases} \frac{1}{2}\ln(M_k) + \frac{\ln(M_i) - \ln(M_j)}{2(M_j - M_i)}M_k + \\ \qquad \frac{M_i\ln(M_j) - M_j\ln(M_i)}{2(M_j - M_i)}, & M_{low} \le M_k \le M_{high} \\ -\infty, & \text{otherwise} \end{cases} \tag{22}$$

where M_i and M_j are the lengths of the two reference species i and j. Despite the fact that M_i and M_j appear explicitly in eq 22, one can prove that they have no effect on the Metropolis acceptance criterion of any variable connectivity MC move that preserves the total number of atoms; consequently, species i and j can be chosen arbitrarily.

That eq 22 indeed generates a uniform distribution of chain lengths for noninteracting grafted chains is demonstrated in Figure 4b. The figure shows the chain length distributions obtained from a MC simulation with grafted freely jointed C_{78} chains (see section 2) where eq 22, and not eq 2, was used for $\boldsymbol{\mu}^*$. The resulting chain length distribution when $\boldsymbol{\mu}^*$ is taken from eq 22 is indeed uniform.

4.2. Grafted Polymer Melts in the Bulk. The general methodology presented in section 3 defining the relationship between chain length distribution and chemical potential spectrum $\boldsymbol{\mu}^*$ is tested here in simulations in the bulk with grafted polymer melts of a

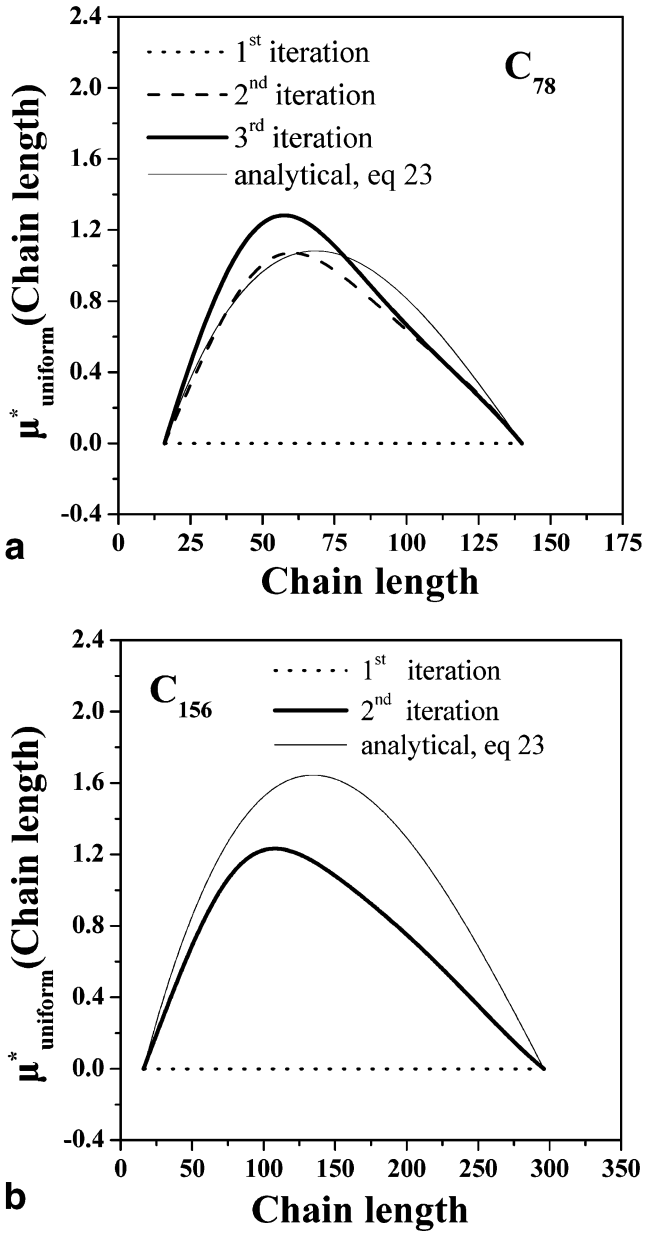

Figure 5. (a) Convergence of the spectrum of chain relative chemical potentials with iteration number for the C_{78} PE melt grafted at $\sigma = 2.62$ nm^{-2}. The prescribed chain length distribution is uniform in the interval [C_{16}, C_{140}] [$T = 450$ K, $P = 0$ atm]. Also shown in the figure is the spectrum $\boldsymbol{\mu}^*$ obtained from eq 23 for the free energy ΔF, proposed by the analytical brush theories.[10−11] (b) Same as in part a but for the C_{156} PE melt grafted at $\sigma = 1.75$ nm^{-2}. The prescribed chain length distribution is uniform in the interval [C_{16}, C_{296}].

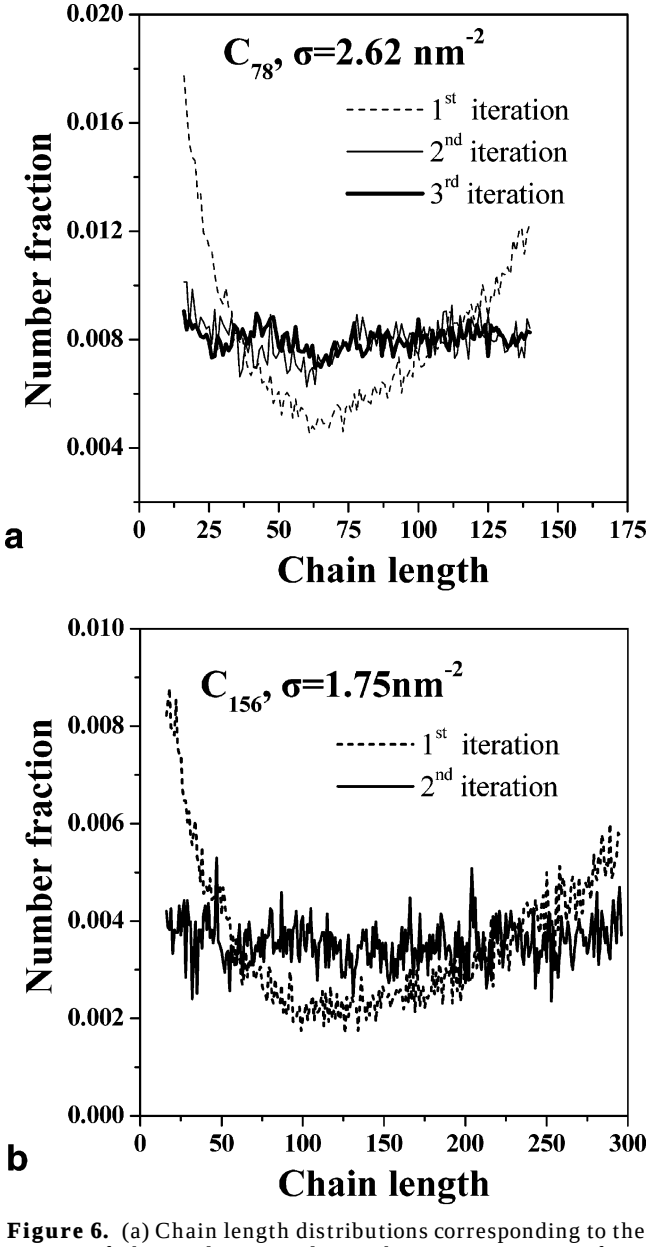

Figure 6. (a) Chain length distributions corresponding to the spectra of chemical potentials $\boldsymbol{\mu}^*$ shown in Figure 5a from EBMC simulations with the grafted C_{78} PE melt ($T = 450$ K, $P = 0$ atm, $\psi = 0.8$). (b) Same as in part a but for the grafted C_{156} PE melt ($T = 450$ K, $P = 0$ atm, $\psi = 0.9$).

precisely known chain length distribution. For simplicity, we restrict ourselves to the case where the prescribed distribution should be uniform. Figure 5a,b presents the convergence of the profile $\boldsymbol{\mu}^*$ with iteration number, from EBMC simulations with the C_{78} and C_{156} PE melt systems discussed in section 2 at grafting densities $\sigma = 2.62$ and 1.75 nm^{-2}, respectively. The evolution of the corresponding chain length distributions is shown in Figure 6a,b. In these figures, each iteration (with the chemical potential spectrum borrowed from the previous step) corresponds to a new-full length simulation. Since the MW distribution responds quite fast to the imposed spectrum $\boldsymbol{\mu}^*$, about 100 million MC steps are enough for each such intermediate simulation run to equilibrate. Figures 5 and 6 show that the convergence properties of the proposed method are very satisfactory: three iterations are enough to determine $\boldsymbol{\mu}^*$ such that the resulting chain length distribution is exactly uniform.

Also shown in Figure 5a,b are the corresponding $\boldsymbol{\mu}^*$ profiles obtained by invoking the expression for $\Delta F = F - F_0 = F_{\text{grafted}} - F_{\text{free}}$ proposed by Milner et al.[10] and Birshtein et al.:[11]

$$\Delta F(N_1, N_2, .., N_m) = \frac{N_{\text{ch}}}{3} A_0 \sigma^2 \sum_{j=1}^{m} \left[(M_j - M_{j-1}) \left(1 - \sum_{i=0}^{j-1} \frac{N_i}{N_{\text{ch}}} \right)^3 \right] \quad (23)$$

$$M_0 \equiv 0, \quad N_0 \equiv 0$$

N_i/N_{ch} in eq 23 is equal to the partial surface coverage φ_i of chains of length M_i, $\varphi_i = \sigma_i/\sigma$, while A_0 is a constant

independent of chain length with dimensions such that the product $A_0\sigma^3$ expresses energy per unit area. Inserting eq 23 into eq 15 gives the following set of nonlinear algebraic equations for the relationship between $\boldsymbol{\mu}^*$ and chain length distribution:

$$\xi_o \equiv 0$$

$$\frac{\xi_m}{N_{ch}} \equiv 1$$

$$\ln(\xi_{j+1} - \xi_j) - \ln(\xi_j - \xi_{j-1}) + \beta A_o \sigma^2 \left(1 - \frac{\xi_j}{N_{ch}}\right)^2 - \lambda\left(\frac{1}{N_{ch}}\right) + \beta\mu^*_j - \beta\mu^*_{j+1} = 0 \quad (24a)$$

$$\sum_{j=1}^{m} M_j \frac{(\xi_j - \xi_{j-1})}{N_{ch}} = \tilde{N}$$

written in terms of the variables ξ_j (j=1, ..., m) defined as

$$\xi_j = \sum_{i=1}^{j} N_i, \text{ and } \xi_m = N_{ch} \quad (24b)$$

If a uniform distribution is specified, eq 24 is solved analytically to give

$$\beta\mu^*_k = -\frac{\beta A_o \sigma^2}{3} \frac{(M_{high} - M_k)^3}{(M_{high} - M_{low} + 1)^2} + \lambda_1 M_k + \lambda_2 \quad (25)$$

with the values of the constants λ_1 and λ_2 being uniquely determined by the lengths M_i and M_j of the two reference species.

Figure 5a,b demonstrates that the predictions of eq 25 deviate from the numerical results for both C_{78} and C_{156} PE melts investigated; however, they are qualitatively correct. This conclusion is drawn by noticing that (a) the analytical and the numerical curves in Figure 5a,b have the same shape, and (b) eq 24 can faithfully fit the chain length distributions obtained from the EBMC simulations for $\boldsymbol{\mu}^* = 0$. This is demonstrated in Figure 7 presenting the chain length distributions obtained from eq 24 with $\boldsymbol{\mu}^* = 0$ for the grafted C_{156} PE melt at $\sigma = 1.75$ nm^{-2}, as a function of their width. The curves have been drawn for a value of the parameter βA_0 on the order of 0.01 and are highly nonuniform, sharing many similarities with those predicted from the atomistic EBMC simulations (shown by the open symbols): (a) the shorter and longer molecular lengths are favored, and (b) they develop asymmetrically around the mean chain length weighting the shorter species.

The examples discussed in sections 4.1 and 4.2 demonstrate the ability of the new simulation scheme introduced in this work to accurately specify the chemical potential spectrum $\boldsymbol{\mu}^*$ such that a well-defined chain length distribution is obtained or strictly preserved in the course of simulations with multicomponent inhomogeneous or anisotropic systems. In addition to providing a recipe for controlling chain length polydispersity, the new method offers a means of (a) estimating the dependence of the system free energy on chain length distribution, (b) testing the validity of corresponding analytical expressions proposed in the literature, and (c) quantifying the effect of polydispersity and

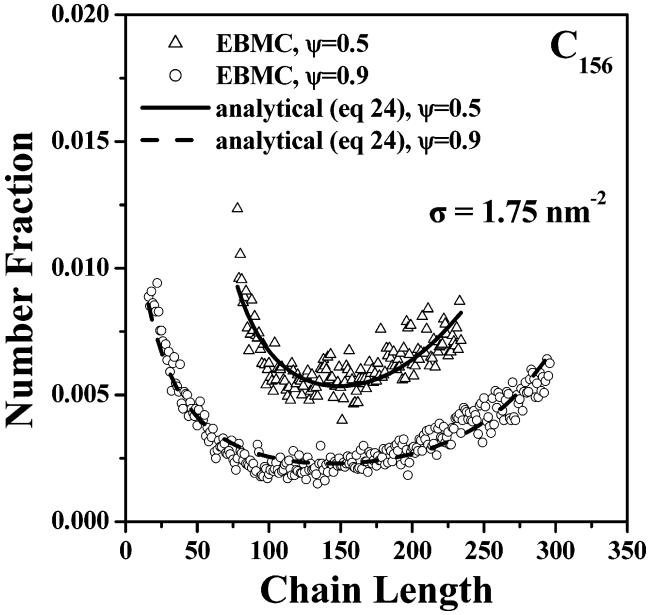

Figure 7. Chain length distributions predicted by the EBMC method with a grafted C_{156} PE melt (T = 450 K, P = 0 atm, $\boldsymbol{\mu}^*$ = 0) and fittings with the analytical expression, eq 24. Two pairs of curves are shown, corresponding to ψ = 0.5 and 0.9, respectively.

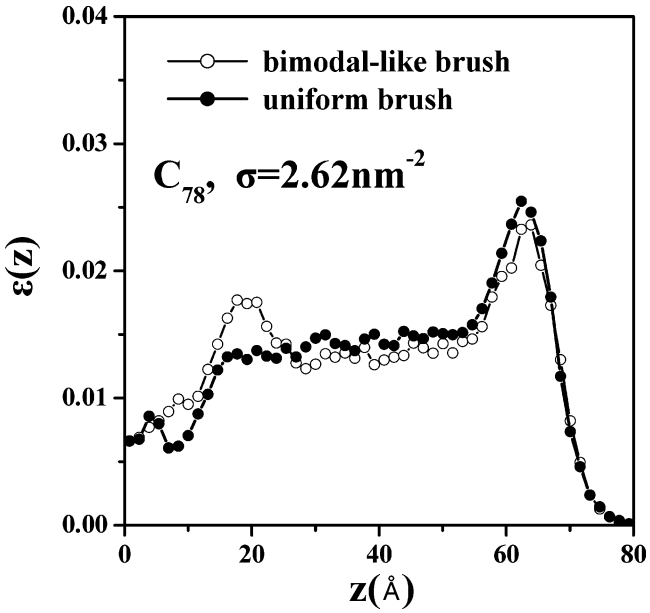

Figure 8. Comparison of the chain free-end distribution function $\epsilon(z)$ as obtained from the EBMC simulations with the C_{78} melt grafted at 2.62 nm^{-2} for (a) $\boldsymbol{\mu}^* = 0$ (bimodal-like brush) and (b) the $\boldsymbol{\mu}^*$ profile that generates a uniform MW distribution.

MW distribution on the interfacial properties of the system. For grafted polymer melts, such a study will be the subject of a future communication. Preliminary simulation runs, however, show that the MW distribution can have a nonnegligible influence on the interfacial profiles of these melts. This is illustrated, for example, in Figures 8 and 9, presenting the profiles of the chain free-end distribution function $\epsilon(z)$ and second-rank bond order parameter $\langle P_2(\cos(\theta))\rangle$, for the bimodal-like and the uniform brushes, respectively. On the other hand, there exist properties, such as the local melt density and consequently the average brush height, whose values are insensitive to the MW distribution. All these will

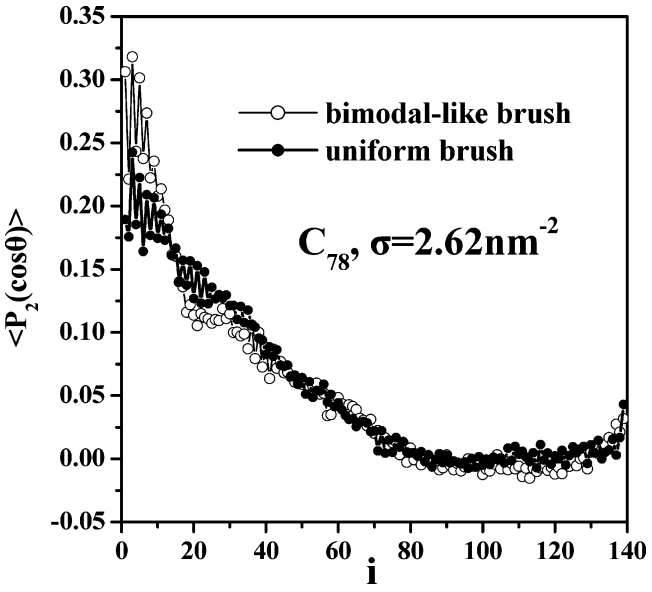

Figure 9. Same as in Figure 8 but for the $\langle P_2(\cos\theta)\rangle$ C−C bond order parameter as a function of bond position i along the chain backbone.

be discussed in a forthcoming article where the interfacial properties of grafted melts characterized by different MW distributions (including strictly monodisperse systems, simulated with the double bridging MC algorithm,[3] as well) are compared with each other in detail.

5. Conclusions

The work presented here generalizes and extends the original formulation of variable connectivity methods by Pant and Theodorou[1] for the atomistic simulation of bulk polydisperse polymer melts to inhomogeneous and/or anisotropic systems, wherein system energetics is fully present. In the new work, not only combinatorial considerations but also entropic/enthalpic effects are explicitly accounted for in the formulation of the relationship between chain length distribution and chain chemical potential spectrum. The new scheme is iterative and combines the capability of newly developed chain connectivity-altering stochastic algorithms (to vigorously sample the configurational space of long-chain polymer systems) with the numerical solution to a set of nonlinear algebraic equations in order to get at the desired relationship between μ^* and prescribed MW distribution.

Two test cases were considered in the present paper: In the first, the spectrum of relative chemical potentials $\mu^* = 0$ was mapped onto a chain length distribution for a system of (a) noninteracting grafted chains modeled as freely jointed chains and (b) atomistically detailed grafted polymer melts. For a free melt, setting $\mu^* = 0$ generates a uniform distribution of chain lengths. Interestingly enough, the resulting MW distribution for grafted systems is highly nonuniform, exhibiting maximum values at the ends of the distribution, i.e., for the shorter and longer chains allowed in the simulation. For two PE melts simulated, C_{78} and C_{156}, it was seen that, with increasing grafting density σ, the extent of the deviation of the resulting distribution from the uniform case is large enough for the grafted melt to assume a bimodal-like structure.

In the second case, the inverse problem was studied, namely the specification of the chemical potential spectrum μ^* that generates a uniform distribution of chain lengths. This latter problem was again addressed for (a) a system of noninteracting grafted chains and (b) a grafted polymer melt brush in the strongly stretched regime. The success of the inverse mapping was directly verified in simulations with polydisperse model systems of grafted C_{78} and C_{156} PE melts: For all grafting densities assumed, the generated chain length distribution was kept uniform exactly as prescribed by the imposed chemical potential spectrum.

The predictions of the new method were also discussed in connection with an expression for the Helmholtz free energy of an end-grafted brush (written as a function of grafting density and melt polydispersity) derived from analytical, SCF theories.

The new method can be used as a guide for the design and efficient implementation of simulation strategies for modeling not only polymer brushes but also a broader class of polymer systems where anisotropy is present. Oriented polymer melts, multicomponent polymer mixtures adsorbed on a surface, self-assembled monolayers, multiphase systems, and conformationally asymmetric polymer blends can be addressed. Developing more accurate analytical, SCF theories for these complex systems could also benefit from the new methodology.

Acknowledgment. K.Ch.D. is grateful to Dr. Alexandros Vanakaras for many helpful discussions in the course of this work. The home institute, ICE/HT-FORTH, is thanked for a generous allocation of CPU time.

References and Notes

(1) Pant, P. V. K.; Theodorou, D. N. *Macromolecules* **1995**, *28*, 7224.
(2) Mavrantzas, V. G.; Boone, T. D.; Zervopoulou, E.; Theodorou, D. N. *Macromolecules* **1999**, *32*, 5072.
(3) Karayiannis, N. Ch.; Mavrantzas, V. G.; Theodorou, D. N. *Phys. Rev. Lett.* **2002**, *88*, 105503. Karayiannis, N. Ch.; Giannousaki, A. E.; Mavrantzas, V. G.; Theodorou, D. N. *J. Chem. Phys.* **2002**, *117*, 5465.
(4) Harmandaris, V. A.; Mavrantzas, V. G.; Theodorou, D. N. *Macromolecules* **1998**, *31*, 7934; **2000**, *33*, 8062.
(5) Harmandaris, V. A.; Mavrantzas, V. G.; Theodorou, D. N.; Kröger, M.; Ramírez, J.; Öttinger, H. C.; Vlassopoulos, D. *Macromolecules* **2003**, *36*, 1376.
(6) Daoulas, K. Ch.; Terzis, A. F.; Mavrantzas, V. G. *J. Chem. Phys.* **2002**, *116*, 11028.
(7) Mavrantzas, V. G.; Theodorou, D. N. *Macromolecules* **1998**, *31*, 6310.
(8) Mavrantzas, V. G.; Öttinger, H. C. *Macromolecules* **2002**, *35*, 960.
(9) Daoulas, K. Ch.; Mavrantzas, V. G.; Photinos, D. J. *J. Chem. Phys.* **2003**, *118*, 1521.
(10) Milner, S. T.; Witten, T. A.; Cates, M. E. *Macromolecules* **1989**, *22*, 853.
(11) Birshtein, T. M.; Liatskaya, Yu. V.; Zhulina, E. B. *Polymer* **1990**, *31*, 2185.
(12) Doi, M.; Edwards, S. F. *The Theory of Polymer Dynamics*; Oxford University Press: New York, 1989.
(13) DiMarzio, E. A. *J. Chem. Phys.* **1965**, *42*, 2101.

MA021570H